

# Squeezing phase diffusion

Simone Cialdi,<sup>1,2</sup> Edoardo Suerra,<sup>1,2</sup> Stefano Olivares,<sup>1,2</sup> Stefano Capra,<sup>1,2</sup> and Matteo G. A. Paris<sup>1,2</sup>

<sup>1</sup>*Dipartimento di Fisica “Aldo Pontremoli”, Università degli Studi di Milano, I-20133 Milano, Italia*

<sup>2</sup>*INFN, Sezione di Milano, I-20133 Milano, Italia*

(Dated: October 13, 2021)

We address the use of optical parametric oscillator (OPO) to counteract phase-noise in quantum optical communication channels, and demonstrate reduction of phase diffusion for coherent signals travelling through a suitably tuned OPO. In particular, we theoretically and experimentally show that there is a threshold value on the phase-noise, above which OPO can be exploited to “squeeze” phase noise. The threshold depends on the energy of the input coherent state, and on the relevant parameters of the OPO, i.e. gain and input/output and crystal loss rates.

## I. INTRODUCTION

The encoding of information onto the phase of an optical signal represents a basic building block for quantum enhanced metrology and communication [1–9]. In particular, protocols based on coherent phase-shift-keyed signals are useful in those scenarios where single photons and entanglement may not be the optimal choice, as it happens in free-space communication. In those cases, the major obstacle to fully exploit the advantages of quantum measurements, thus beating the shot-noise limit, is phase noise due to phase diffusion [10–16].

Besides trying to avoid phase noise, a question thus arises on whether, and how, it may be possible to contrast and counteract the effects of phase diffusion, and to decrease its detrimental effect on the coherence of the signal. In this framework, a natural choice to hamper phase diffusion is to use phase-sensitive amplification, as that provided by optical parametric oscillators (OPOs) in the degenerate regime. Despite the simplicity of the underlying idea the use of OPO to *squeeze* phase diffusion did not receive much attention in the past. The reason is twofold: on the theoretical side, the existence of quantum limits to amplification suggests that no full compensation of noise is possible [17–21]. On the experimental side, *seeding* a quantum amplifier with a phase diffused state in order to compensate the noise is not a trivial task. Likewise, achieving the necessary level of pump phase stabilization may be challenging.

In this paper, thanks to an active stabilisation scheme of our OPO cavity and to a novel technique for pump stabilisation, we have been able to explore experimentally the use of optical parametric oscillator (OPO) to counteract phase-noise, and to demonstrate reduction of phase diffusion for coherent signals. In particular, we theoretically and experimentally show that there is a threshold value on the phase-noise, above which OPOs may be exploited to effectively *squeeze* phase noise. As we will see, the noise threshold depends on the amplitude of the input signal, and on the relevant parameters of the OPO, i.e. gain and input/output and crystal loss rates.

The paper is structured as follows. In Section II, we introduce notation and discuss the effect of an OPO on a phase-diffused coherent signal. In Section III, we briefly describe our experimental setup and present our results, showing that above a given threshold of the phase diffusion amplitude, OPO may be indeed exploited to squeeze phase noise. Section IV

closes the paper with some concluding remarks.

## II. PHASE DIFFUSION AND OPO

Let us consider a coherent state  $|\beta e^{i\varphi}\rangle$ , with  $\beta \in \mathbb{R}_+$  undergoing phase diffusion. The evolved state may be written as [14, 22]

$$\varrho = \int d\phi g_\sigma(\phi) |\beta e^{i\phi}\rangle \langle \beta e^{i\phi}|, \quad (1)$$

where  $g_\sigma(\phi) = (2\pi\sigma^2)^{-\frac{1}{2}} \exp\{-\frac{1}{2}\phi^2/\sigma^2\}$  and we refer to  $\sigma$  as to the amplitude of the phase diffusion (see Fig. 1). An estimate of the phase  $\varphi$  may be obtained from the expectations of the two orthogonal quadratures  $x = a + a^\dagger$  and  $y = i(a^\dagger - a)$ , where  $a$  and  $a^\dagger$  are the creation and annihilation operators,  $[a, a^\dagger] = 1$

$$\hat{\varphi} = \tan^{-1} \frac{\langle y \rangle}{\langle x \rangle}. \quad (2)$$

The uncertainty in the estimate  $\hat{\varphi}$  is thus given by namely:

$$\begin{aligned} \text{var}[\hat{\varphi}] &= \left( \frac{\langle y \rangle}{\langle x \rangle^2 + \langle y \rangle^2} \right)^2 \text{var}[x] \\ &+ \left( \frac{\langle x \rangle}{\langle x \rangle^2 + \langle y \rangle^2} \right)^2 \text{var}[y]. \end{aligned} \quad (3)$$

For a coherent signal  $\text{var}[x] = \text{var}[y] = 1$

$$\text{var}[\hat{\varphi}] = \frac{1}{4\beta^2}, \quad (4)$$

that scales, as expected, as the inverse of the energy  $|\beta|^2$  of the input coherent state. Notice that we estimate phase by two measurements performed on two copies of the input state [23] (thanks to stability of the scheme). Let us now consider a coherent signal undergoing phase diffusion, and for the sake of simplicity let us assume that  $\varphi = 0$ , i.e.,  $\beta \in \mathbb{R}$  and  $\beta > 0$ . In this case we have:

$$\langle x \rangle = 2|\beta|e^{-\sigma^2} \quad \text{and} \quad \langle y \rangle = 0, \quad (5)$$

and:

$$\text{var}[x] = 1 + 2\beta^2 \left(1 - e^{-\sigma^2}\right)^2, \quad (6)$$

$$\text{var}[y] = 1 + 2\beta^2 \left(1 - e^{-2\sigma^2}\right). \quad (7)$$

Note that  $\text{var}[x] \leq \text{var}[y]$ . It is straightforward to show that:

$$\text{var}[\hat{\varphi}] = \frac{\cosh(\sigma^2) + (1 + 4\beta^2) \sinh(\sigma^2)}{4\beta^2} \geq \frac{1}{4\beta^2} \quad (8)$$

In Fig. 1 we compare a coherent state with its phase diffused counterpart.

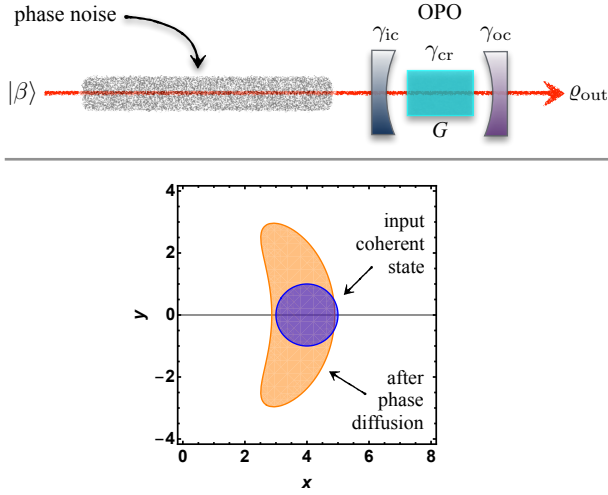


FIG. 1: (Upper panel): After the phase diffusion the noisy signal enters an OPO characterised by the gain  $G$  and by the input,  $\gamma_{ic}$ , output,  $\gamma_{oc}$  and crystal  $\gamma_{cr}$  loss rates. (Lower panel): phase-space representation a coherent state  $|\beta\rangle$  (blue) and its phase diffused counterpart (orange). We set  $\beta = 2$  and  $\sigma = \pi/4$ . It is clear the effect of phase noise on the uncertainty of the  $x$  and  $y$  quadratures.

Let us now assume that after the phase diffusion process the degraded state passes through an OPO as sketched in the upper panel of Fig. 1. The OPO can be characterised by the gain and the input and output parameters,  $\eta_{in}$  and  $\eta_{esc}$ , respectively, which summarise the effect of the input and output couplers transmissivity and the internal losses [24]. The gain can be written as  $G = (1 - d)^{-2}$ , where  $d = \sqrt{P/P_{th}}$ , where  $P$  is the pump power and  $P_{th}$  the OPO power threshold; the input and output parameters depends on the input ( $\gamma_{ic}$ ) and output ( $\gamma_{oc}$ ) loss rates of the input and output couplers, respectively, but also on the loss rate due to the OPO crystal ( $\gamma_{cr}$ ). Overall, we have:

$$\eta_{in} = \frac{\gamma_{ic}}{\gamma} \quad \text{and} \quad \eta_{esc} = \frac{\gamma_{oc}}{\gamma}, \quad (9)$$

where we introduced  $\gamma = \gamma_{ic} + \gamma_{oc} + 2\gamma_{cr}$ . In the following we will focus on the effect of the OPO on the first and second moments of the quadratures relevant for our analysis. We begin our study assuming as input a coherent state  $|\beta e^{i\phi}\rangle$  (without phase noise). Lengthy but straightforward calculations lead to

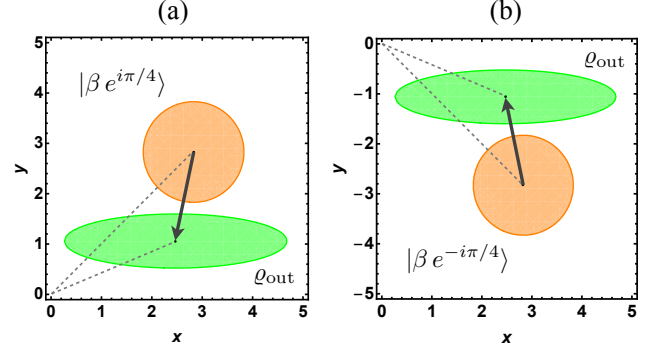


FIG. 2: Phase-space representation a coherent  $|\beta e^{i\varphi}\rangle$  state before (blue) and after the evolution through the OPO (green). We set  $\beta = 2$  and two values of the phase: (a)  $\varphi = \pi/4$  and (b)  $\varphi = -\pi/4$ . In both the cases the phase approaches 0 after the evolution. We used the realistic OPO parameters  $d = 0.40$  ( $G = 2.78$ ),  $\eta_{in} = 0.08$  and  $\eta_{esc} = 0.87$ .

the following results (we choose the OPO pump phase such to amplify the  $x$  quadrature):

$$X \equiv \langle x \rangle = \frac{\sqrt{4\eta_{in}\eta_{esc}}}{1-d} 2\beta \cos \varphi, \quad (10a)$$

$$Y \equiv \langle y \rangle = \frac{\sqrt{4\eta_{in}\eta_{esc}}}{1+d} 2\beta \sin \varphi, \quad (10b)$$

and

$$\Sigma_x^2(\eta_{esc}, d) \equiv \text{var}[x] = 1 + \eta_{esc} \frac{4d}{(1-d)^2} \geq 1, \quad (11a)$$

$$\Sigma_y^2(\eta_{esc}, d) \equiv \text{var}[y] = 1 - \eta_{esc} \frac{4d}{(1+d)^2} \leq 1. \quad (11b)$$

In Fig. 2 we show the effect of the OPO on a coherent state for a particular choice of the involved parameters. It is worth noting that the presence of the OPO reduces the phase shift of the state: this effect will be fundamental to reduce the phase diffusion.

When phase noise affects the propagation of the coherent state before the OPO, the evolved state is given by Eq. (1). By using the results of Eqs. (10) and (11) it is easy to find the new mean values of the relevant quadratures and their variances, namely (we set  $\varphi = 0$ ):

$$\langle x \rangle = \alpha_x e^{-\sigma^2/2} \quad \langle y \rangle = 0, \quad (12a)$$

and

$$\text{var}[x] = \Sigma_x^2 + \alpha_x^2 e^{-\sigma^2} [\cosh(\sigma^2) - 1], \quad (13a)$$

$$\text{var}[y] = \Sigma_y^2 + \alpha_y^2 e^{-\sigma^2} \sinh(\sigma^2), \quad (13b)$$

where:

$$\alpha_x \equiv \alpha_x(\beta, \eta_{in}, \eta_{esc}, d) = \frac{\sqrt{4\eta_{in}\eta_{esc}}}{1-d} 2\beta, \quad (14a)$$

$$\alpha_y \equiv \alpha_y(\beta, \eta_{in}, \eta_{esc}, d) = \frac{\sqrt{4\eta_{in}\eta_{esc}}}{1+d} 2\beta, \quad (14b)$$

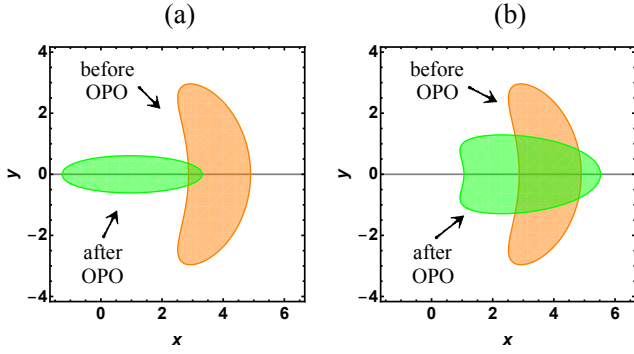


FIG. 3: Phase-space representation of a phase diffused coherent state (orange) and its state  $\rho_{\text{out}}$  after the evolution through the OPO (green). We set  $\beta = 2$ ,  $\varphi = 0$  for the input coherent state and  $\sigma = \pi/4$  for the phase noise amplitude and  $d = 0.4$  ( $G = 2.78$ ). For the input and output parameters we used the realistic values (a)  $\eta_{\text{in}} = 0.01$ ,  $\eta_{\text{esc}} = 0.93$  and (b)  $\eta_{\text{in}} = 0.08$ ,  $\eta_{\text{esc}} = 0.87$ . We can see that the uncertainty of the  $y$  quadrature is reduced after the evolution through the OPO.

whereas  $\Sigma_x^2$  and  $\Sigma_y^2$  are given in Eqs. (11). In Fig. 3 we can see how a phase diffused coherent state is modified by the evolution through the OPO. In order to assess the reduction of

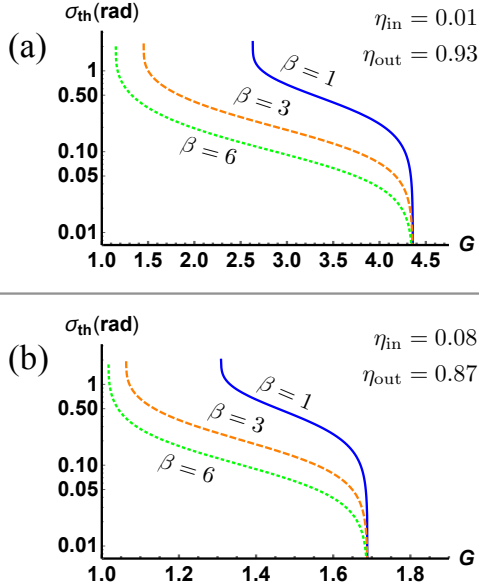


FIG. 4: Threshold value  $\sigma_{\text{th}}$  of the phase noise as a function of the OPO gain  $G = (1 - d)^{-2}$  for different values of the input coherent state  $\beta$ : if  $\sigma > \sigma_{\text{th}}$  the OPO reduces the phase noise. The input and output parameters of the panels are  $\eta_{\text{in}} = 0.01$  and  $\eta_{\text{esc}} = 0.93$  (top panel) and  $\eta_{\text{in}} = 0.08$  and  $\eta_{\text{esc}} = 0.87$  (right panel).

phase diffusion, we use the previous results to evaluate  $\hat{\varphi}$  and  $\text{var}[\hat{\varphi}]$  given in Eqs. (2) and (3). In particular, for the variance we find:

$$\text{var}[\hat{\varphi}] = \frac{\Sigma_y^2 + \alpha_y^2 e^{-\sigma^2} \sinh(\sigma^2)}{\alpha_x^2 e^{-\sigma^2}}. \quad (15)$$

By comparing the variance (15) and the one obtained without the OPO, namely, Eq. (8), we can find a threshold value  $\sigma_{\text{th}}$

of the phase noise amplitude above which phase diffusion can be reduced, namely:

$$\sigma_{\text{th}}(\beta, \eta_{\text{in}}, \eta_{\text{esc}}, d) = \sqrt{\log \left[ \frac{\sqrt{2}\beta \sqrt{\alpha_x^2 - \alpha_y^2}}{\sqrt{\alpha_x^2 + 2\beta^2(\alpha_x^2 - \alpha_y^2 - 2\Sigma_x^2)}} \right]}. \quad (16)$$

In Fig. 4 we plot the threshold  $\sigma_{\text{th}}$  as a function of the OPO gain  $G = (1 - d)^{-2}$  for different values of the involved parameters. We can see that, for a fixed choice of the involved parameters, there exists a maximum value of  $G$  above which the OPO always reduces phase noise.

### III. EXPERIMENTAL RESULTS

Theoretical predictions have been tested using the experimental scheme depicted in Fig. 5. The setup allows us to generate and manipulate displaced-squeezed states. In particular, we have control not only on both the amplitude and phase of the states, but also on the gain  $G$  and the pump phase. The setup is described in detail in [25] and consists of different stages: a Laser source (LASER), a state generation and manipulation stage (SG) and an homodyne detector (HD). A home-made 1064 nm wavelength Nd:YAG laser internally frequency doubled at 532 nm serves both as the input seed and the pump beam for the Optical Parametric Oscillator (OPO). In particular, from the infrared output of the laser we generate two different beams by a polarising beam splitter: one is used as the local oscillator (LO) for the homodyne detection, while the other is sent to the SG.

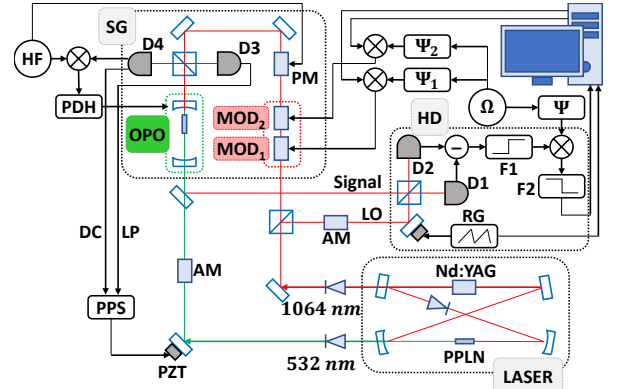


FIG. 5: Schematic diagram of the experimental setup. The main source is the Nd:YAG laser internally frequency-doubled, while OPO is in the state generation stage (SG). States are revealed by a homodyne detector (HD). Generation and detection are fully controlled by a computer.

OPO consists in a linear cavity with a free spectral range of 3.270 GHz. A 10 mm-long MgO:LiNbO<sub>3</sub> crystal with anti-reflection coating is inserted inside the cavity. The losses related to the crystal are  $\Delta = 2.42 \times 10^{-3}$ . We used two different configurations A and B for the OPO. In configuration A the input mirror has a reflectivity  $R_{\text{ic,A}} = 0.999$  with a radius

of curvature of 10 mm, while the output mirror has a reflectivity  $R_{oc} = 0.917$  with a radius of curvature of 25 mm, leading to  $\eta_{in,A} = 0.008$  and  $\eta_{esc,A} = 0.937$ , with a measured cavity total transmissivity  $T_A = 0.029$ . In configuration B the input mirror has a reflectivity  $R_{ic,B} = 0.9925$ , and the output mirror is the same as A, both with the same radii of curvature of A, leading to  $\eta_{in,B} = 0.079$  and  $\eta_{esc,B} = 0.871$ , with a measured cavity total transmissivity  $T_B = 0.26$ . The role of the transmissivities will be clear later. The cavity is actively stabilized using the Pound-Drever-Hall (PDH) technique [26] by means of a phase modulator (PM) placed along the SG beam, which generates two 116 MHz sidebands around the laser frequency. Coherent states are generated exploiting the combined effect of two optical modulators (MOD1 and MOD2) placed before the OPO. A proper choice of their modulations allows us to generate an arbitrary coherent state on the sidebands at 3 MHz for seeding the OPO [25, 26]. Amplitude and phase values are set on demand by a computer.

In order to effectively amplify a certain quadrature with the OPO, the pump phase  $\Theta$  must be stable over the whole time of the measurement. Therefore, a novel technique for the pump phase stabilization (PPS) has been developed and will be described in detail in a forthcoming work [27], whereas in the following we highlight its main elements. In our stabilization technique, the field  $E_{r,tot}$  reflected by the OPO can be exploited as an error signal for the stabilization of  $\Theta$ . We note that the field  $E_{r,tot}$  is the sum of the field  $E_r$ , directly reflected by the input mirror, and the field  $E_t$  transmitted by the cavity through the input mirror. The laser and the field generated by down conversion by the pump interact inside the cavity and their interaction leads to constructive or destructive interference depending on the pump phase  $\Theta$ . Since  $E_r$  and  $E_t$  are  $\pi$ -shifted, in the first case  $E_t$  increases and  $E_{r,tot}$  decreases, while in the second case  $E_t$  decreases and  $E_{r,tot}$  increases. This can be summarized as  $E_{r,tot} = E_{r,tot}(\Theta)$ , thus in order to access the information about  $\Theta$  we measure the corresponding power  $P_{r,tot}$  with the DC output of the detector  $D_4$  (see Fig. 5). Finally, the obtained error signal is properly manipulated with a PID and applied to a piezoelectric actuator which can change  $\Theta$ . At the moment the total bandwidth of the PPS is around 1 kHz, thus we can compensate pump phase fluctuations of at most that frequency.

The effect of the OPO on a phase-diffused coherent state has been tested directly by generating a rapid sequence of three coherent states: one with 0-phase shift and two with a  $\pm 40^\circ$ -phase shift. Indeed, considering the Eqs. (10), if the phase shift before OPO is  $\varphi = \theta_0$ , then after OPO we have

$$\frac{\langle y \rangle}{\langle x \rangle} = \frac{1-d}{1+d} \tan \varphi, \quad (17)$$

leading to the simple relation

$$\tan \theta_d = \frac{1-d}{1+d} \tan \theta_0 \quad (18)$$

where  $\theta_d$  and  $\theta_0$  refer to the case with and without OPO respectively. We performed a tomography of every state, both with and without the OPO. Results are shown in the upper

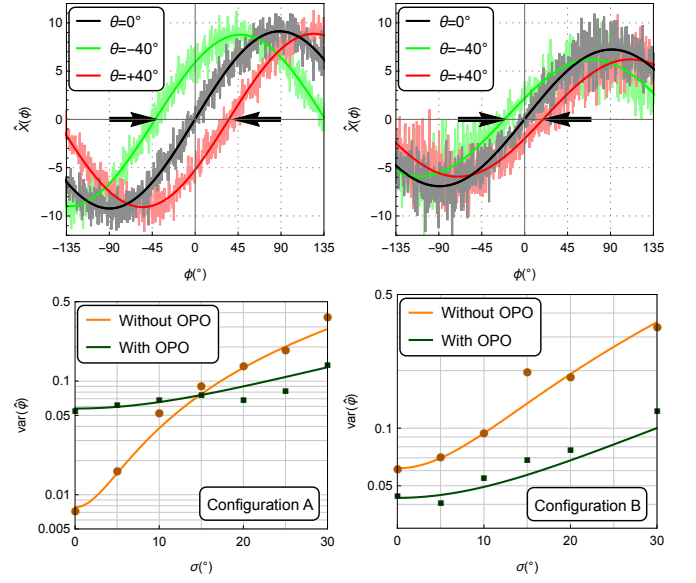


FIG. 6: (Upper panels): Tomography of a sequence of three  $40^\circ$ -shifted coherent states (left) and relative effect of OPO (right). The marked line is the mean value of each state. Notice the reduction of the phase shift as marked by the arrows. Here the system is in configuration A, but the amplitude of the states is different in the two cases without and with OPO ( $\beta = 4.5$  and  $\beta_{OPO} = 2.0$  with  $G = 3.1$ , respectively). (Lower panels): Variance of  $\varphi$  in function of the phase diffusion for the configurations A (left) and B (right). Theoretical curves (lines) fit well the experimental points. Notice the presence of the threshold at  $14.8^\circ$  in configuration A.

panels of Fig. 6. In order to highlight the effect of the OPO on the phase shift, we used two different amplitudes for the cases with and without the OPO and this is possible as the reduction of the phase shifts does not depend on the  $\beta$ s [it is clear from Eq. (18)]. In particular the system was in configuration A, with  $\beta = 4.5$  without OPO and  $\beta_{OPO} = 2.0$  with OPO. In this last case the gain was  $G = 3.1$ , leading to  $d = 0.43$ . Results show that the phase shift is reduced from  $\theta_0 = 40^\circ$  to a measured  $\theta_{d,ex} = 20^\circ$ , while the theoretical value calculated with  $d$  is  $\theta_{d,th} = 18.4^\circ$ .

In our experiments, we generated the phase-diffused coherent states by modulating their phases with a suitable Gaussian distribution [28] and we evaluated  $\text{var}[\hat{\varphi}]$  of Eq. (15) with and without OPO for different values of the phase diffusion  $\sigma$  in both configurations A and B. For practical reasons, in the measurements without OPO we did not physically remove it from the setup, but we increased the amplitude of the coherent state by a factor  $1/\sqrt{T}$  with respect to the case of squeezed coherent, in order to compensate the effect of the cavity transmissivity  $T$ . That is why we have measured transmissivities. Of course, pump was turned off during these measurements. In order to obtain  $\text{var}[\hat{\varphi}]$ , we measured  $\langle x \rangle$ ,  $\langle y \rangle$ ,  $\text{var}[x]$  and  $\text{var}[y]$  and we used Eq. (3). We made measurements for different values of the phase diffusion  $\sigma$ . The theoretical expectation has been obtained directly using Eq. (15), where we considered the experimental values for  $\Sigma_y$ ,  $\beta$  and  $G$ , from which we calculated  $\alpha_x$  and  $\alpha_y$ . Finally, the threshold  $\sigma_{th}$  has been calculated by Eq. (16). Both the experimental points

and the theoretical previsions are shown in the lower panels of Fig. 6 for the two configurations. In particular, in configuration A we have  $\beta_A = 5.70$  and  $G_A = 2.75$ , with a theoretical threshold  $\sigma_{th} = 14.8^\circ$  perfectly compatible to experimental points. In configuration B we have  $\beta_B = 2.05$ ,  $G_B = 3.12$  and there is no threshold, so the use of the OPO is convenient for every phase diffusion amplitude.

#### IV. CONCLUSIONS

In this paper, we have exploited our innovative OPO scheme to address the use of phase-sensitive amplification to counteract phase-noise in quantum phase channels. Our results demonstrate the reduction of phase diffusion for coherent

signals travelling through a suitably tuned OPO. More generally, we have shown that there is a threshold value on the phase-noise, above which OPO can be exploited to squeeze phase noise. The threshold depends on the energy of the input coherent state, and on the relevant parameters of the OPO. Our results may be exploited to enhance quantum phase communication channels and for state preparation in quantum metrological schemes.

#### Acknowledgments

This work has been partially supported by FNP TEAM project "Quantum Optical Communication Systems" and by UniMI project PSR2017-DIP-008.

- 
- [1] C. M. Caves, *Quantum-mechanical noise in an interferometer*, Phys. Rev. D. **23**, 1693 (1981) .
- [2] M. Holland, and K. Burnett, *Interferometric detection of optical phase shifts at the heisenberg limit*, Phys. Rev. Lett. **71**, 1355 (1993) .
- [3] V. Giovannetti, S. Lloyd, and L. Maccone, *Quantum metrology*, Phys. Rev. Lett. **96**, 010401 (2006) .
- [4] V. Giovannetti, S. Lloyd, and L. Maccone, *Advances in quantum metrology*, Nat. Photonics **5**, 222 (2011) .
- [5] R. Demkowicz-Dobrzanski, U. Dorner, B. J. Smith, J. S. Lundeen, W. Wasilewski, K. Banaszek, and I. A. Walmsley *Quantum phase estimation with lossy interferometers*, Phys. Rev. A **80**, 013825 (2009) .
- [6] B. Escher, R. de Matos Filho, and L. Davidovich, *General framework for estimating the ultimate precision limit in noisy quantum-enhanced metrology*, Nat. Phys. **7**, 406 (2011) .
- [7] R. Chaves, J. Brask, M. Markiewicz, J. Koodyski, and A. A. Acn, *Noisy metrology beyond the standard quantum limit*, Phys. Rev. Lett. **111**, 120401 (2013) .
- [8] A. Smirne, J. Koodyski, S. F. Huelga, and R. Demkowicz-Dobrzanski, *Ultimate precision limits for noisy frequency estimation*, Phys. Rev. Lett. **116**, 120801 (2016) .
- [9] S. Daryanoosh, S. Slussarenko, D. W. Berry, H. M. Wiseman, and G. J. Pryde, *Experimental optical phase measurement approaching the exact Heisenberg limit*, Nat. Comm. **9**, 4606 (2018) .
- [10] M. Bina, A. Allevi, M. Bondani, and S. Olivares, *Phase-reference monitoring in coherent-state discrimination assisted by a photon-number resolving detector*, Sci. Rep. **6**, 26025 (2016) .
- [11] C. Wittmann, U. L. Andersen, M. Takeoka, D. Sych, and G. Leuchs, *Demonstration of coherent-state discrimination using a displacement-controlled photon-number-resolving detector*, Phys. Rev. Lett. **104**, 100505 (2010) .
- [12] C. R. Müller, M. A. Usuga, C. Wittmann, M. Takeoka, C. Marquardt, U. L. Andersen, and G. Leuchs, *Quadrature phase shift keying coherent state discrimination via a hybrid receiver*, New. J. Phys. **14**, 083009 (2012) .
- [13] S. Izumi, M. Takeoka, K. Ema, and M. Sasaki, *Quantum receivers with squeezing and photon-number-resolving detectors for M-ary coherent state discrimination*, Phys. Rev. A **86**, 042328 (2012) .
- [14] M. G. Genoni, S. Olivares, and M. G. A. Paris, *Optical phase estimation in the presence of phase diffusion*, Phys. Rev. Lett. **106**, 153603 (2011) .
- [15] C. Wittmann, M. Takeoka, K. N. Cassemiro, M. Sasaki, G. Leuchs, and U. L. Andersen, *Demonstration of near-optimal discrimination of optical coherent states*, Phys. Rev. Lett. **101**, 210501 (2008) .
- [16] K. Tsujino, D. Fukuda, G. Fujii, S. Inoue, M. Fujiwara, M. Takeoka, and M. Sasaki, *Quantum receiver beyond the standard quantum limit of coherent optical communication*, Phys. Rev. Lett. **106**, 250503 (2011) .
- [17] W. H. Louisell, A. Yariv, and A. E. Siegman, *Quantum fluctuations and noise in parametric processes I*, Phys. Rev. **124**, 1654 (1961); J. P. Gordon, W. H. Louisell, and L. R. Walker, *Quantum fluctuations and noise in parametric processes II*, Phys. Rev. **129**, 481 (1963).
- [18] H. Heffner, *The fundamental noise limit of linear amplifiers*, Proc. IRE **50**, 1604 (1962).
- [19] H. A. Haus, and J. A. Mullen, *Quantum noise in linear amplifiers*, Phys. Rev. **128**, 2407 (1962).
- [20] C. M. Caves, *Quantum limits on noise in linear amplifiers*, Phys. Rev. D **26**, 1817 (1982).
- [21] C. M. Caves, J. Combes, Z. Jiang, and S. Pandey, *Quantum limits on phase-preserving linear amplifiers*, Phys. Rev. A **86**, 063802 (2012).
- [22] M. G. Genoni, S. Olivares, D. Brivio, S. Cialdi, D. Cipriani, A. Santamato, S. Vezzoli, and M. G. A. Paris, *Optical interferometry in the presence of large phase diffusion*, Phys. Rev. A **85**, 043817 (2012).
- [23] S. Olivares, *Quantum optics in the phase space - A tutorial on Gaussian states*, Eur. Phys. J. Special Topics **203**, 3-24 (2012).
- [24] H.-A. Bachor, and T. C. Ralph, *A Guide to Experiments in Quantum Optics* (Wiley-VCH, Weinheim, 2004).
- [25] A. Mandarino, M. Bina, C. Porto, S. Cialdi, S. Olivares, and M.G.A. Paris, *Assessing the significance of fidelity as a figure of merit in quantum state reconstruction of discrete and continuous variable systems*, Phys. Rev. A **93**, 062118 (2016).
- [26] S. Cialdi, C. Porto, D. Cipriani, S. Olivares, and M.G.A. Paris, *Full quantum state reconstruction of symmetric two-mode squeezed thermal states via spectral homodyne detection and a state-balancing detector*, Phys. Rev. A **93**, 043805 (2016).
- [27] S. Cialdi, E. Suerra, and S. Olivares, *Pump phase stabilization in an Optical Parametric Oscillator*, in preparation.

- [28] S. Olivares, S. Cialdi, F. Castelli, and M. G. A. Paris, *Homodyne detection as a near-optimum receiver for phase-shift keyed binary communication in the presence of phase diffusion*, Phys. Rev. A **87**, 050303(R) (2013).